

Identification of pyrvinium pamoate as an anti-tuberculosis agent *in vitro* and *in vivo* by SOSA approach amongst known drugs

Qing Guan^{a,b*}, Lingjun Zhan^{c*}, Zhi-Hao Liu^{a*}, Qin Pan^{a*}, Xu-Lin Chen^d, Zhen Xiao^a, Chuan Qin^c and Xiao-Lian Zhang^{a,e}

^aHubei Province Key Laboratory of Allergy and Immunology and Allergy Department of Zhongnan Hospital, Department of Immunology, Wuhan University School of Basic Medical Sciences, Wuhan, People's Republic of China; ^bDepartment of Laboratory Medicine, Xiangyang Central Hospital, Affiliated Hospital of Hubei University of Arts and Science, Xiangyang, People's Republic of China; ^cInstitute of Laboratory Animal Science, Chinese Academy of Medical Sciences (CAMS), Beijing Key Laboratory for Animal Models of Emerging and Reemerging Infectious; Tuberculosis (TB) Center, Chinese Academy of Medical Sciences, Beijing, People's Republic of China; ^dWuhan Institute of Virology, Chinese Academy of Sciences, Wuhan, People's Republic of China; ^eState Key Laboratory of Virology, Medical Research Institute Wuhan University School of Medicine, Wuhan, People's Republic of China

ABSTRACT

Tuberculosis (TB), caused by *Mycobacterium tuberculosis* (*M.tb*) bacteria, is a leading infectious cause of mortality worldwide. The emergence of drug-resistant *M. tb* has made control of TB more difficult. The selective optimization of side activities (SOSA) approach uses old drugs for new pharmacological targets. In the present study by using SOSA approach, we have successfully identified pyrvinium pamoate (PP) which is capable of inhibiting the growth of mycobacteria, including *M. tb* H37Rv, *Mycobacterium smegmatis*, Bacille Calmette-Guérin (BCG), *M. tb* H37Ra, and drug-resistant *M. tb* clinical isolates *in vitro* from 1280 known drugs library. The MIC₉₉ of PP, the minimum inhibitory concentration that inhibits more than 99% of *M. tb* H37Rv and the drug-resistant *M. tb* clinical isolates, ranges from 1.55 to 4.8 µg/mL. Importantly, PP could reduce the bacterial colony-forming units (CFUs) in lung, spleen and liver tissues, and effectively inhibit inflammatory response in *M. tb* H37Rv, multidrug-resistant (MDR) *M. tb* and extensively drug-resistant (XDR) *M.tb*-infected mice. Our results clearly show that the PP has the potential application for treatment of TB.

ARTICLE HISTORY Received 31 October 2019; Revised 13 January 2020; Accepted 19 January 2020





KEYWORDS *Mycobacterium tuberculosis*; anti-TB drug screening; pyrvinium pamoate; selective optimization of side activities approach; multidrug-resistant *M. tb*

Introduction

Mycobacterium tuberculosis (*M. tb*), a causative pathogen of tuberculosis (TB), is one of the most dangerous bacteria in the world [1]. TB is the world's major public health problem with high morbidity and mortality [2]. One-third of the world's people are infected with *M. tb*, 8–9 million people suffering from TB each year, and approximately 1.2 million people died from TB in 2018 [2]. *M. tb* strains mainly infect lung, but also infect many other organs such as kidney, brain, spine, lymph nodes, causing extrapulmonary TB [3]. First-line treatments of TB consist of isoniazid (INH), rifampicin (RIF), pyrazinamide (PZA) and ethambutol (EMB) during the first 2 months, continuing with INH and RIF for another 4 months [4]. However, the emergence of multidrug-resistant (MDR) *M.tb* and extensively drug-resistant (XDR) *M.tb* makes the control of TB more difficult. MDR-TB is

defined as TB resistant to at least INH and RIF. XDR-TB is defined as MDR-TB plus resistance to any fluoroquinolone and at least one of three injectable drugs (kanamycin, amikacin and capreomycin). Because of limited treatment options for MDR-TB and XDR-TB, they pose additional challenges for global TB control efforts. It is urgent to search for new drugs for treatment of TB, including MDR-TB and XDR-TB.

Because high cost and long approval process limits the clinical application of new anti-TB drugs, the selective optimization of side activities (SOSA) was developed as an innovative strategy to solve these problems. Using the SOSA approach, new potential pharmacological targets of old approved drugs may be identified [5,6]. The safety and pharmacokinetic properties of these old drugs have been well evaluated in humans and animals, so the new biological activities of these approved drugs can be more

CONTACT Xiao-Lian Zhang  chuanqin@vip.sina.com  Hubei Province Key Laboratory of Allergy and Immunology, Department of Immunology, Wuhan University School of Basic Medical Sciences, Donghu Road 185#, Wuhan 430071, People's Republic of China; Chuan Qin  chuanqin@vip.sina.com  Institute of Laboratory Animal Science, Chinese Academy of Medical Sciences (CAMS), Beijing Key Laboratory for Animal Models of Emerging and Reemerging Infectious; Tuberculosis (TB) Center, Chinese Academy of Medical Sciences, Beijing, People's Republic of China

*These authors contributed equally to this work.

 Supplemental data for this article can be accessed at <https://doi.org/10.1080/22221751.2020.1720527>

© 2020 The Author(s). Published by Informa UK Limited, trading as Taylor & Francis Group, on behalf of Shanghai Shangyixun Cultural Communication Co., Ltd
This is an Open Access article distributed under the terms of the Creative Commons Attribution License (<http://creativecommons.org/licenses/by/4.0/>), which permits unrestricted use, distribution, and reproduction in any medium, provided the original work is properly cited.

rapidly and easily applied in clinical practice than new drugs. SOSA has been used in the development of new anti-malarial, antibacterial and antiviral drugs [7-11]. In the present study, we used the SOSA approach to screen out a new anti-*M. tb* drug, pyrvinium pamoate (PP), a US Food and Drug Administration (FDA)-approved drug from the MicroSource (Gaylordsville, CT) library consisting of 1280 drugs and compounds. We have identified that PP is capable of inhibiting multiple mycobacterial species (including *M. tb* H37Rv, H37Ra, BCG and drug-resistant *M. tb* clinical isolates) growth *in vitro* and can protect mice against *M. tb* H37Rv, MDR *M. tb* and XDR *M.tb* infection.

Materials and methods

Bacteria, cells and medium

Mycobacterium smegmatis (*M. smegmatis*, strain ATCC 70084), *M. bovis* BCG (strain ATCC 35734) and *M. tb* H37Rv (strain ATCC 93009) were from Animal Experimental Center of Wuhan University or China National Institute for the Control of Pharmaceutical and Biological Products [12]. *M. tb* H37Ra strain was kindly provided by Prof. Xiong-Lin Fan (Huazhong University of Science and Technology, Wuhan, China). MDR *M. tb* strain 94789 and XDR *M. tb* strain 8462 were provided by China Food and Drug Administration Institute. The MDR *M. tb* strain 94789 is resistant to INH and RIF. The XDR *M. tb* strain 8462 is resistant to INH, RIF, ofloxacin, and streptomycin (STR). Drug-sensitive *M.tb* clinical isolates and drug-resistant *M. tb* clinical isolates were provided by Wuhan Medical Treatment Center. *M. smegmatis* was cultured in Luria-Bertani (LB) medium with 0.05% Tween 80 or onto Middlebrook 7H10 solid growth medium (BD Biosciences, NJ, USA). Other mycobacterial strains were grown in Middlebrook 7H9 (or 7H10) broth (BD Biosciences, NJ, USA) supplemented with 10% oleic acid-albumin-dextrose-catalase (OADC, BD Biosciences, NJ, USA) and 0.05% Tween 80.

Murine macrophage RAW264.7 cells were purchased from China Center for Type Culture Collection (CCTCC). To prepare murine peritoneal macrophages, thioglycolate-elicited macrophages were prepared by injecting mice with 3.5 mL of 3% sterile thioglycolate media (BD Biosciences, NJ, USA) [12,13]. After 5 days, peritoneal cells were collected by lavage. The cells were cultured overnight and non-adherent cells were removed. The adherent macrophages were collected and stained with anti-F4/80 antibody for purity analysis. F4/80⁺ macrophages were greater than 90% of total cells (data not shown). The cells were cultured in DMEM supplemented with 10% FBS, 100 U/mL penicillin and 100 µg/mL STR.

Antibiotic and chemicals

The drugs and chemical compounds applied in the library screening were kindly provided by Prof. Xu-Lin Chen (Wuhan Institute of Virology, Chinese Academy of Sciences, China). The library (MicroSource Discovery Systems, Inc. Gaylordsville, CT, USA) consists of 1280 drugs and bioactive compounds. Most of these drugs in this library are FDA-approved, but all have known biological activity. Some drugs, which have not received FDA approval, are approved for clinical use in other countries [14]. These 1280 drugs and bioactive compounds were added to 96 cell culture plates (16 plates of 80 each.) using their laboratory instruments (Echo Sonic Micropipical System).

RIF (CAS#54-85-3), meclizine hydrochloride (CAS#71-58-9), adiphenine hydrochloride (CAS#50-42-0) and BZK (CAS#8001-54-5) were purchased from Wuhan Yi Tai Technology, China. Suloctidil (CAS#54063-56-8) and meclizine hydrochloride (CAS# 31884-77-2) were purchased from Shanghai Tao Su Biochemical Technology Co. Ltd. China. Teniposide (CAS#29767-20-2), isoproterenol hydrochloride (CAS#51-30-9) and doxorubicin (CAS#23214-92-8) were purchased from Shanghai Han Hong Biological Technology Co. Ltd. China. Pyrvinium pamoate (CAS#3546-41-6) was purchased from Dalian Meilun Biotechnology Co. Ltd, China.

Screening

During the library screening, *M. smegmatis* was diluted to 2.5×10^6 colony-forming units (CFUs)/mL and 200 µL of bacteria solution were added to 96-well cell culture plates in the presence of 25 µM of each candidate drugs and compounds from the library. After 2-day culture, the A_{600} values of bacterial solutions were measured by a microplate reader (SpectraMax[®] i3, Molecular Devices, LLC, CA, USA). To further confirm the inhibitory effects of selected candidate drugs PP, benzalkonium chloride (BZK), meclizine hydrochloride, suloctidil, doxorubicin, teniposide, isoproterenol hydrochloride, medroxyprogesterone acetate and adiphenine hydrochloride on *M. smegmatis* growth, the bacteria were cultured in the presence of various concentrations of the selected candidate drugs (0–10 µg/mL), and A_{600} values and CFUs of *M. smegmatis* were determined.

To assess the effects of the candidate drugs on growth of BCG and *M. tb* H37Ra, these mycobacteria were diluted to 2.5×10^6 CFUs/mL in 4 mL of 7H9 liquid medium containing various concentrations of PP, BZK, meclizine hydrochloride, suloctidil, doxorubicin and teniposide respectively (0–10 µg/mL). To assess the effects of PP on the growth of *M. tb* H37Rv, *M. tb* H37Rv was diluted to 2.5×10^6 CFUs/mL in 4 mL of 7H9 liquid medium containing various

concentrations of PP. After 30-day culture, the A_{600} values of bacterial solutions were measured. In positive control group, *M. tb* H37Rv was cultured without the drugs. 7H9 liquid medium was used as medium control. Inhibition % = $(A_{600 \text{ experimental group}} - A_{600 \text{ medium control}}) / (A_{600 \text{ positive control}} - A_{600 \text{ medium control}})$. The half maximal inhibitory concentration (IC_{50}) values were calculated using GraphPad 6.0 software (Graphpad software, San Diego, CA). The MIC_{99} values were calculated using the statistical package IBM SPSS Statistics software (SPSS) (IBM Corp., Armonk, NY, USA).

To assess the effects of PP on the growth of drug-sensitive *M. tb* and drug-resistant *M. tb* clinical isolates, these clinical isolates were diluted to 2.5×10^6 CFUs/mL in 4 mL of 7H9 liquid medium containing various concentrations of PP (0–10 $\mu\text{g/mL}$). After 15-day culture, the A_{600} values of bacterial solutions were measured by Maxwell concentration detector in Wuhan Medical Treatment Center.

Cell viability analysis

Cell viability analysis was performed by CCK-8 assay according to the manufacturer's recommendations (Beyotime, Shanghai, China). Murine peritoneal macrophages and RAW264.7 cells were seeded in 96-well plates (2×10^4 cells/100 μL /well). The cells were cultured in the presence of various concentrations of PP (0.1–10 $\mu\text{g/mL}$) for 24 h. CCK-8 solution (10 μL /well, Beyotime, Shanghai, China, #C0038) was added to each well. The plates were incubated for 2 h and A_{450} values were measured using a microplate reader. CC_{50} (drug concentration required to reduce cell viability by 50%) of PP was calculated using GraphPad 6.0 software. The selective index (SI) was calculated according to the equation: $SI = CC_{50} / IC_{50}$.

Drug susceptibility testing (DST) and determination of minimum inhibitory concentration (MIC)

DST was performed using MGIT SIRE kit and liquid *Mycobacterium* Growth Indicator Tube system (MGIT) 960 as previously described [15]. In addition to 7H9 liquid medium, the MGIT tube contains an oxygen-quenched fluorochrome, tris 4,7-diphenyl-1,0-phenanthroline ruthenium chloride pentahydrate, embedded in silicone at the bottom of the tube. During bacterial growth within the MGIT tube, the free oxygen is utilized and the intensity of fluorescence from the tubers is directly proportional to the extent of oxygen depletion. Growth of mycobacteria increases the fluorescence. The assessment of drug susceptibility was determined automatically at the point at which the proportional-growth control reached 400 growth units (GU). The instrument declares a tube negative

if it remains negative for six weeks (42 days). In the current study, *M. tb* H37Rv, MDR *M. tb* strain 94789 and XDR *M. tb* strain 8462 were analyzed by DST. These mycobacterial strains were cultured in the presence of INH, RIF or STR. The recommended concentrations were 0.2 $\mu\text{g/mL}$ for INH, 5 $\mu\text{g/mL}$ for RIF and 1 $\mu\text{g/mL}$ for STR.

To determine the MICs of PP against different *M. tb* strains, *M. tb* H37Rv, MDR *M. tb* 94789 and XDR *M. tb* 8462 were cultured in the various concentrations of PP (0.1–3 $\mu\text{g/mL}$). By the use of the automated Bactec MGIT 960 system, all strains were interpreted objectively and the MICs were determined. The lowest concentration of drug that inhibits growth of more than 99 % of the bacterial population was considered to be the MIC_{99} .

Murine TB infection models

Female C57BL/6 mice (6–8 week, 17–19 g, SPF) were purchased from Beijing Charles River Laboratories. The use of these laboratory animals has been approved by the Committee on the Use and Management of Laboratory Animals, Institute of Medical Laboratory Animals, Chinese Academy of Medical Sciences, Beijing (Approval No. ZLJ17002). Animal rearing and experimentation were carried out in the Grade 3 Laboratory of Biosafety, Institute of Medical Laboratory Animals, Chinese Academy of Medical Sciences (ABSL3-059).

Totally 96 female C57BL/6 mice were used and six mice were used for each group. The mice were infected (*i. v.*) with *M. tb* H37Rv (1×10^6 CFUs/mouse), *M. tb* H37Rv 94789 (1×10^4 CFUs/mouse) or *M. tb* H37Rv 8462 (1×10^5 CFUs/mouse) on week –1. After a week of infection (in Week 0), the mice were treated with RIF (20 mg/kg/day, 5 days/week), EMB (100 mg/kg/day, 5 days/week) or PP (0.5 mg/kg/day in Week 1, 1 mg/kg/day in Week 2–5 and 1.5 mg/kg/day in Week 6, 5 days/week) by oral gavage. In EMB + PP combination therapy group, the mice were treated with EMB (100 mg/kg/day, 5 days/week) and PP (0.5 mg/kg/day in Week 1, 1 mg/kg/day in Week 2–5 and 1.5 mg/kg/day in Week 6, 5 days/week). In RIF + PP combination therapy group, the mice were treated with RIF (20 mg/kg/day, 5 days/week) and PP (0.5 mg/kg/day in Week 1, 1 mg/kg/day in Week 2–5 and 1.5 mg/kg/day in Week 6, 5 days/week). After 4 weeks or 6 weeks of therapy treatment, the *M. tb* loads in the lungs, spleens and livers mice were assessed. The sections of lungs, spleens and livers were fixed in 4% paraformaldehyde and pathological sections were examined with hematoxylin–eosin (H&E) staining.

Statistical analysis

Data were analyzed with SPSS software and GraphPad 6.0 software. Differences were considered to be

statistically significant for P -values <0.05 . Statistical significance was determined by Student's t -test or one-way ANOVA followed by Newman–Keuls post hoc test.

Results

Six drugs were selected from a library of 1280 candidates for inhibiting *M. smegmatis* growth in vitro

M. smegmatis has been commonly used to screen new anti-TB drugs due to its rapid growth rate [16]. In the current study, to find a new anti-*M. tb* drug, *M. smegmatis* was firstly used as a target for screening out *M. tb* inhibitors from the 1280 candidate drugs and compounds. *M. smegmatis* was cultured in liquid

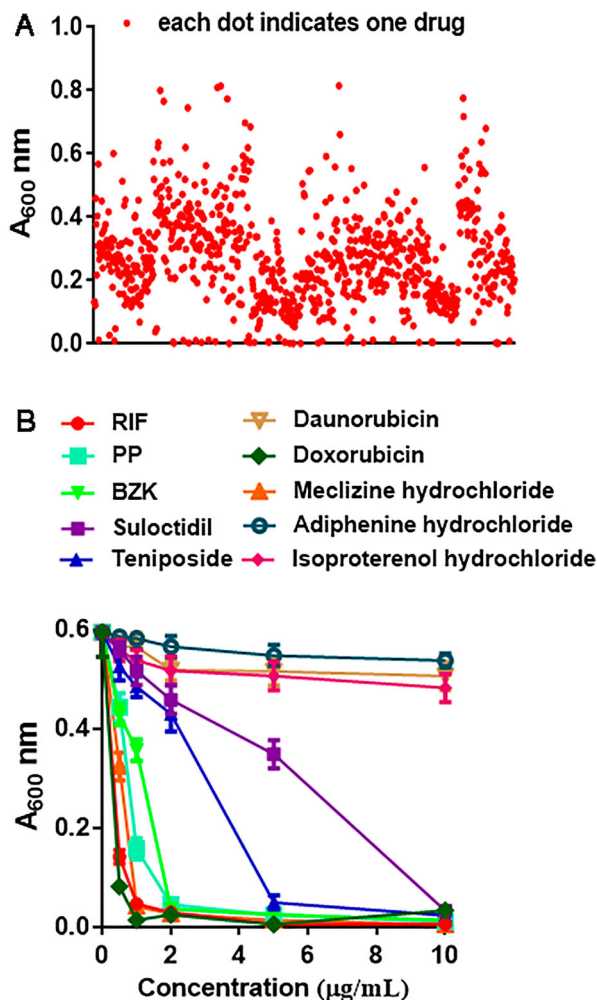


Figure 1. Six drugs are screened out from 1280 candidate drugs for inhibiting *M. smegmatis* growth in vitro. (A) A_{600} values of *M. smegmatis* cultured in the presence of 1280 candidate drugs. The bacteria were cultured in the 7H9 liquid medium containing 25 μM compounds in 96-well cell culture plate. After 48 h culture, the bacterial growth was determined by A_{600} value. (B) A_{600} values of *M. smegmatis* cultured in the presence of various concentrations of the indicated drugs. After 48 h culture, the bacterial growth was determined by A_{600} value. The data in (B) are shown as the means \pm SD ($n=3$).

medium containing 25 μM of each candidate drug, and A_{600} value of *M. smegmatis* was determined to evaluate effects of candidate drugs on bacterial growth (Figure 1(A)). 67 drugs out of the 1280 candidate drugs were shown to inhibit *M. smegmatis* growth. We removed the anti-*M.tb* drugs (including INH, RIF, etc) and toxic compounds (including acetic acid phenyl mercury, thioglycans, etc) from these 67 drugs, and chose nine drugs (Table 1, Supplemental Table 1), including PP, benzalkonium chloride (BZK), meclizine hydrochloride, suloctidil, doxorubicin, teniposide, isoproterenol hydrochloride, medroxyprogesterone acetate and adiphenine hydrochloride, that would be employed in the next round of screen.

To further confirm the inhibitory effects of these candidate drugs, *M. smegmatis* was cultured in liquid medium containing various concentrations of the drugs (0–10 $\mu\text{g/mL}$), and A_{600} value of *M. smegmatis* was determined. Adiphenine hydrochloride, daunorubicin and isoproterenol hydrochloride, have limited inhibitory effects on *M. smegmatis* growth (Figure 1(B)). Six drugs, PP, BZK, meclizine hydrochloride, suloctidil, doxorubicin and teniposide, were shown to inhibit *M. smegmatis* in dose-dependent manner (Figure 1(B)). PP and doxorubicin showed the strongest inhibitory effects on *M. smegmatis* growth. The MIC_{99} values of PP and doxorubicin on *M. smegmatis* were 9 and 5 $\mu\text{g/mL}$, respectively (Table 1).

PP inhibits standard laboratory strain *M. tb* H37Rv growth in vitro

We then assessed the activity of these drugs on growth of BCG, *M. tb* H37Ra and H37Rv. BCG, Bacille Calmette-Guérin, is a live, attenuated vaccine derived from *Mycobacterium bovis*, and *M. tb* H37Ra is an attenuated strain originated from *M. tb*. Both of these *Mycobacteria* are more closely related to the virulent strain *M. tb* H37Rv than *M. smegmatis*. BCG and *M. tb* H37Ra were cultured in the presence of various concentrations of the drugs for 30 days. As shown in Figure 2(A), only two drugs, PP and BZK, inhibited the growth of BCG and *M. tb* H37Ra in a dose-dependent manner, and other four drugs had no inhibitory effect on the growth of BCG and *M. tb* H37Ra.

Table 1. The MIC_{99} values of ten drugs on *M. smegmatis*.

Drugs	MIC_{99} ($\mu\text{g/mL}$)
RIF	5
Doxorubicin	5
Pyrvinium pamoate (PP)	9
Meclizine hydrochloride	10
Benzalkonium chloride (BZK)	>10
Suloctidil	>10
Teniposide	>10
Adiphenine hydrochloride	>10
Daunorubicin	>10
Isoproterenol hydrochloride	>10

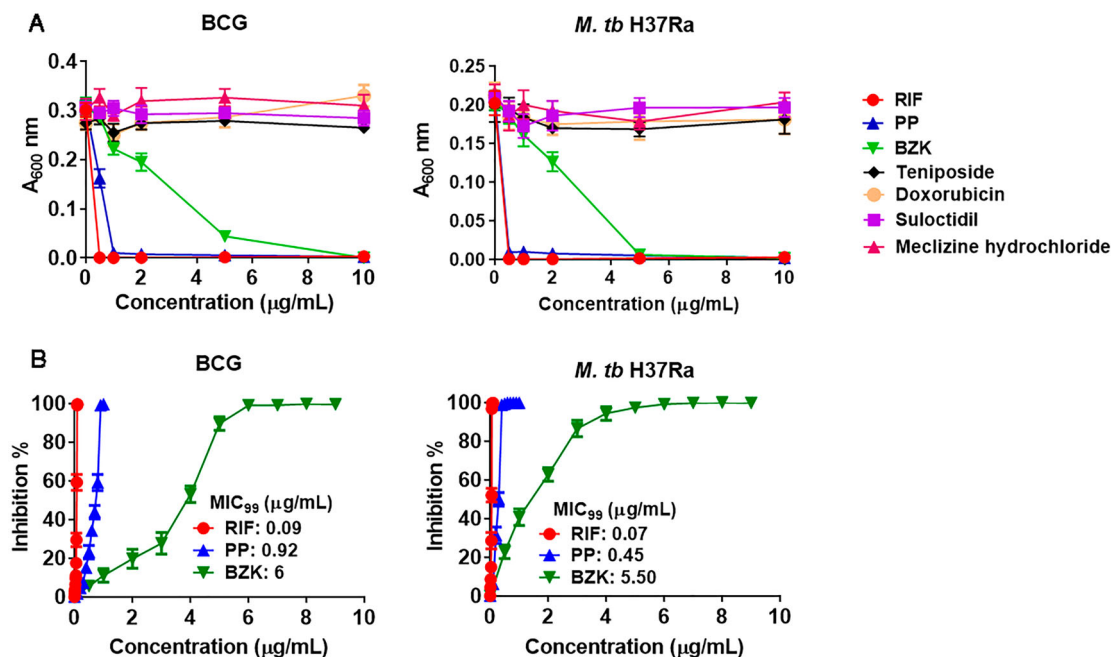


Figure 2. PP inhibits the growth of BCG and *M. tb* H37Ra *in vitro*. (A) and (B) PP and BZK inhibited the growth of BCG and *M. tb* H37Ra. BCG and *M. tb* H37Ra were cultured in the presence of various concentrations of the drugs as indicated for 30 days, and A₆₀₀ values of BCG and *M. tb* H37Ra were determined. In the infection control group, *M. tb* H37Ra was cultured without the drugs. 7H9 liquid medium was used as medium control. (A) A₆₀₀ values of BCG and *M. tb* H37Ra. (B) Inhibition % of BCG and *M. tb* H37Ra by PP and BZK, and MIC₉₉ of PP and BZK. Inhibition % = (A₆₀₀ experimental group - A₆₀₀ medium control) / (A₆₀₀ positive control - A₆₀₀ medium control). All data are shown as the means ± SD (n=3). IC₅₀ values were calculated using GraphPad 6.0 software. The MIC₉₉ values were calculated using the statistical package IBM SPSS Statistics software.

To assess the inhibitory effects of PP and BZK on BCG and *M. tb* H37Ra, the inhibition % of mycobacterial growth and the MIC₉₉ values for PP and BZK were calculated (Figure 2(B) and Table 2). Both PP and BZK significantly inhibited BCG and *M. tb* H37Ra growth in the comparative low concentrations (Figure 2(B) and Table 2). However, BZK showed less effective than RIF, and PP was similar effectiveness as compared to RIF (Figures 2(A,B) and Table 2). The MIC₉₉ values of PP on BCG and *M. tb* H37Ra were 0.92 and 0.45 µg/mL, respectively, which were much lower than those of BZK (6 µg/mL on BCG and 5.5 µg/mL on *M. tb* H37Ra, respectively, Figure 2(B) and Table 2). Therefore, PP was selected and its inhibitory effect on virulent *M. tb* was evaluated in the following experiments.

To assess the inhibitory effects of PP on standard laboratory strain *M. tb* H37Rv, *M. tb* H37Rv was cultured in the presence of various concentrations of PP

for 30 days, and the inhibition % of *M. tb* H37Rv growth and PP MIC₉₉ value were calculated (Figure 3). PP was capable of inhibiting *M. tb* H37Rv growth in a dose-dependent manner, although PP showed a little less effective than RIF (Figure 3). The MIC₉₉ values were 1.65 µg/mL for PP and 0.30 µg/mL for RIF on *M. tb* H37Rv. Therefore, PP has an inhibitory effect on *M. tb* H37Rv growth *in vitro*.

SI value reflects the “fitting” of the drug to the particular target [14]. The higher SI value is, the more suitable the drug for the particular target is. To further

Table 2. The MIC₉₉ values of the selected drugs on BCG and H37Ra.

Drugs	MIC ₉₉ (µg/mL)	
	BCG	H37Ra
RIF	0.2	0.3
PP	0.92	0.45
BZK	6	5.5
Meclizine hydrochloride	>10	>10
Suloctidil	>10	>10
Doxorubicin	>10	>10
Teniposide	>10	>10

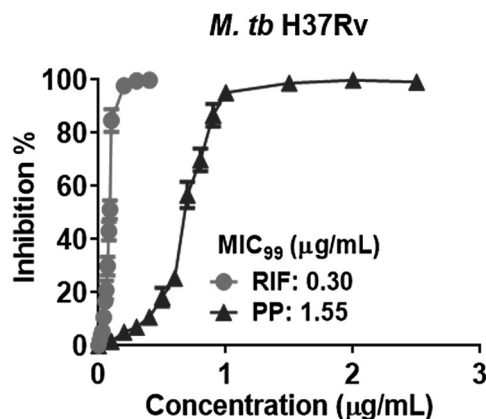


Figure 3. PP inhibits the standard laboratory strain *M. tb* H37Rv growth *in vitro*. *M. tb* H37Rv was cultured in the presence of various concentrations of PP for 30 days, and the A₆₀₀ value of *M. tb* H37Rv was measured, Inhibition % and MIC₉₉ were calculated. The data are shown as the means ± SD (n=3).

Table 3. SI and MIC₉₉ values of PP on Mycobacteria.

Bacteria	IC ₅₀ (µg/mL)	CC ₅₀ (µg/mL)	SI (CC ₅₀ /IC ₅₀)	MIC ₉₉ (µg/mL)
BCG	0.75	2.4	3.2	0.92
<i>M. tb</i> H37Ra	0.3	2.4	8	0.45
<i>M. tb</i> H37Rv	0.65	2.4	3.69	1.55
Drug-sensitive <i>M. tb</i>				
Strain 1	0.60	2.4	4.03	4.8
Strain 2	0.71	2.4	3.4	1.9
Strain 3	0.47	2.4	5.1	4.0
Strain 4	0.43	2.4	5.6	4.5
Strain 5	0.46	2.4	5.2	4.6
MDR <i>M. tb</i>				
Strain 1	0.45	2.4	5.35	4.5
Strain 2	0.39	2.4	6.09	1.9
Strain 3	0.51	2.4	4.66	2.0
Strain 4	0.39	2.4	6.09	4.8
Strain 5	0.71	2.4	4.37	4.6
INH-resistant <i>M. tb</i>				
Strain 1	0.49	2.4	4.89	3.5
Strain 2	0.50	2.4	4.74	4.0
Strain 3	0.80	2.4	2.98	4.8
Strain 4	0.46	2.4	5.17	4.6
Strain 5	0.51	2.4	4.67	1.8
RIF-resistant <i>M. tb</i>				
Strain 1	1.0	2.4	2.4	4.8
Strain 2	0.74	2.4	3.23	2.0

evaluate PP effects on various *M. tb* strains, we calculated the SI values of PP for laboratory strain *M. tb* and clinical *M. tb* isolates. As shown in Table 3, the SI values of PP for laboratory standard strain *M. tb* H37Rv were 3.69, which was lower than that SI values for most of clinical isolates *M. tb* (3.40-6.09). These

results suggested that PP “fits” more selectively to clinical isolates than laboratory strain *M. tb* H37Rv.

PP inhibits growth of both drug-sensitive and drug-resistant *M. tb* clinical isolates in vitro

To assess the inhibitory effect of PP on the clinical isolates of *M. tb*, both drug-sensitive and drug-resistant *M. tb* clinical isolates were employed. The MIC₉₉ values of PP on five drug-sensitive *M. tb* clinical isolates were 4.8, 1.9, 4.0, 4.5 and 4.6 µg/mL, respectively (Figure 4 (A) and Table 3). The MIC₉₉ values of PP on five INH-resistant *M. tb* clinical isolates were 3.5, 4.0, 4.8, 4.6 and 1.8 µg/mL, respectively (Figure 4(B) and Table 3). The MIC₉₉ values of PP on two RIF-resistant *M. tb* clinical isolates were 4.8 and 2.0 µg/mL (Figure 4 (C) and Table 3). The MIC₉₉ values of PP on five MDR *M. tb* were 4.5, 1.9, 2.0, 4.8 and 4.6 µg/mL, respectively (Figure 4(D) and Table 3). These results strongly demonstrated that PP inhibited growth of both drug-sensitive and drug-resistant *M. tb* clinical isolates.

PP inhibits *M. tb* h37Rv infection in mice

Next, we assessed the protective effects of PP in a mouse model against *M. tb* infection. The mice were

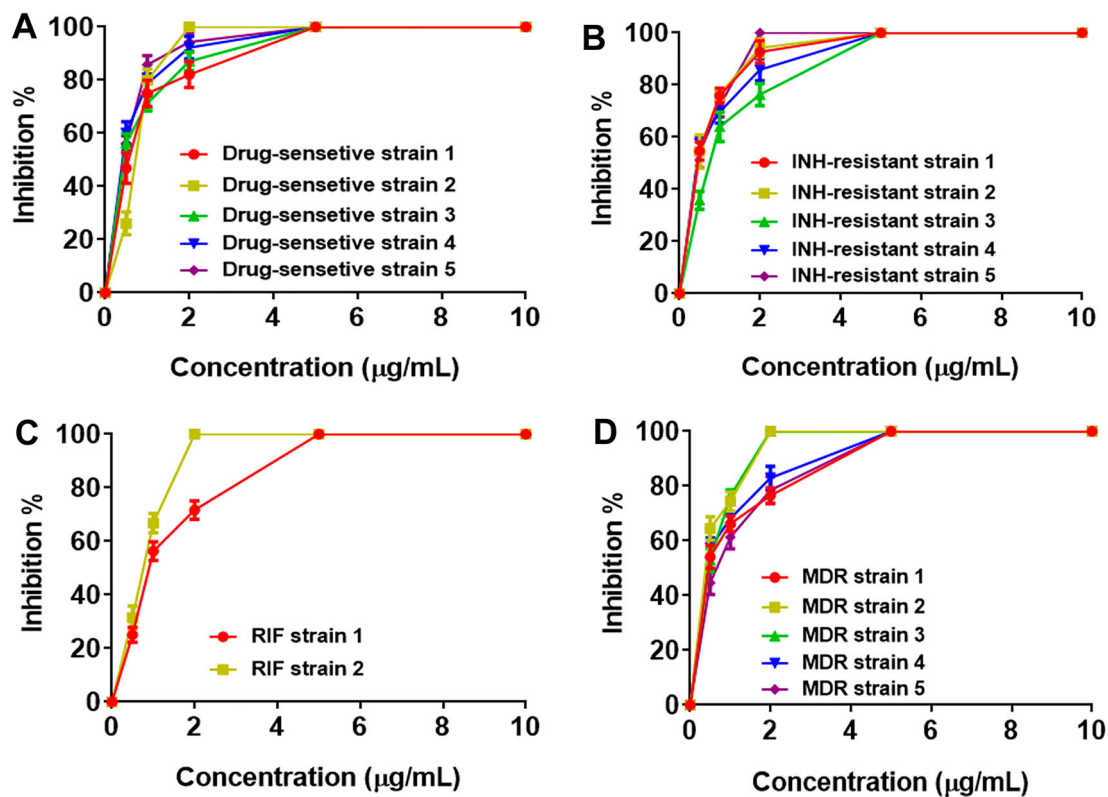


Figure 4. PP inhibits both drug-sensitive and drug-resistant *M. tb* clinical isolates growth *in vitro*. Drug-sensitive and drug-resistant *M. tb* clinical isolates were cultured in the presence of various concentrations of PP for 15 days, and the A₆₀₀ values of *M. tb* clinical isolates were measured. Inhibition % and MIC₉₉ were calculated. (A) Inhibition % of drug-sensitive *M. tb* clinical isolates (strain 1–5) and MIC₉₉ values of PP; (B) Inhibition % of INH-resistant *M. tb* clinical isolates (strain 1–5) and MIC₉₉ values of PP; (C) Inhibition % of RIF-resistant *M. tb* clinical isolates (strain 1 and 2) and MIC₉₉ values of PP; (D) Inhibition % of MDR-resistant *M. tb* clinical isolates (strain 1–5) and MIC₉₉ values of PP. The data in (A)–(D) are shown as the means ± SD (n = 3).

i.v. infected with *M. tb* H37Rv on Week -1. These mice were treated with PP, RIF or PP plus RIF weekly from week 0 to week 6. After 4 weeks or 6 weeks of the treatment, as shown in Figure 5(A-C), PP treatment significantly reduced the bacterial CFUs in lung, spleen and liver tissues compared with PBS control group, indicating that PP treatment inhibited *M. tb* H37Rv growth *in vivo* (Figure 5(A-C)). However, PP did not have a more effective antibacterial effect than RIF. PP combined with RIF treatment did not further reduce the CFUs in mice, indicating no synergic effects between PP and RIF (Figure 5(A-C)).

Histological analysis revealed that *M. tb* infection caused severe pathological changes and inflammation response in lung, spleen and liver tissues in the *M. tb* H37Rv group. After treatment with PP, RIF and PP plus RIF, the pulmonary lesion and inflammation alleviated, especially the 6-week treatment with PP markedly and effectively reduced lesion and inflammatory in the lungs compared with the other groups (Figure 5(D-F), Supplemental Figure 1). Granulomas, inflammatory cells infiltration and thickening of bronchial alveolar wall were observed in the lungs in the PBS control group (Figure 5(D)). Disorganization of white pulp (WP) and red pulp (RP) in spleens and hepatocyte lesion were also observed in *M. tb* H37Rv plus PBS control group (Figure 5(E,F)). In PP, RIF and PP

plus RIF groups, the WP and RP were clearly evident and lymphoid hyperplasia occurred in spleens, indicating the active proliferation of immune cells after the drug treatment (Figure 5(E)). Compared with the PBS control group, 6-week treatment of PP and PP plus RIF ameliorated the hepatocyte swelling, indicating that PP has a potential advantage of liver protection over RIF (Supplemental Figure 1). These results strongly demonstrated that PP treatment reduced severe pathological changes and inflammatory response, and inhibited *M. tb* H37Rv infection in mice.

PP inhibits MDR *M.tb* and XDR *M.tb* infection in mice

To assess whether PP had protective effects on drug-resistant *M. tb* infection *in vivo*, the MDR *M. tb* 94789 and XDR *M. tb* 8462 were used. Before mice infection, we determined that the MDR *M. tb* strain 94789 was resistant to INH and RIF, and the XDR *M.tb* strain 8462 was resistant to INH, RIF, ofloxacin, and streptomycin (STR). The results showed that the MIC₉₉ of PP against *M. tb* H37Rv, *M. tb* 94789 and *M. tb* 8462 were 1.5 µg/mL, 3 µg/mL, and 0.75 µg/mL, respectively (Supplemental Table 2).

In the mouse model of *M. tb* 94789 infection, the mice were *i.v.* infected with *M. tb* 94789 on week -1.

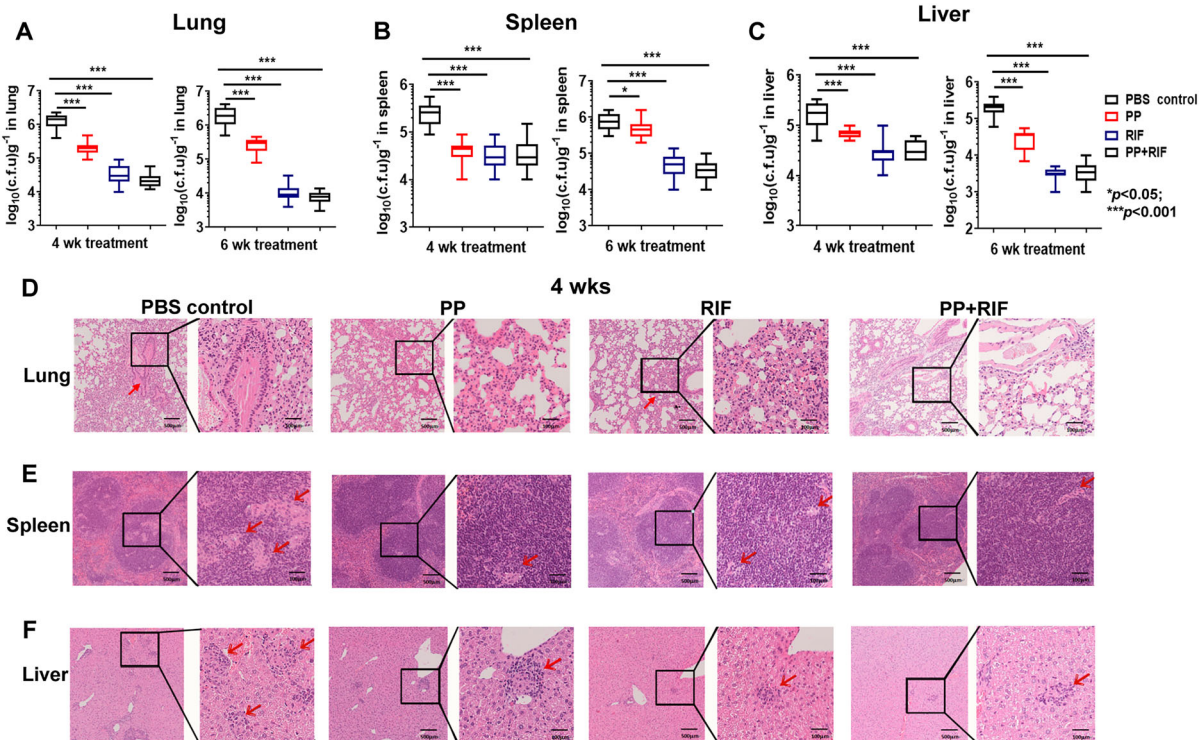


Figure 5. PP inhibits *M. tb* H37Rv growth in mice. The mice were infected (*i. v.*) with *M. tb* H37Rv (1×10^6 CFU/mouse), and subjected to treatment with PP, RIF or PP in combination with EBM. After 4 weeks or 6 weeks of therapy treatment, the bacterial loads in the lungs (A), spleens (B) and livers (C) were assessed. The pathological sections of lungs (D), spleens (E) and livers (F), obtained 4 weeks after therapy treatment, were examined with H&E and evaluated by light microscopy. The data in (A)–(C) are shown as the means \pm SD ($n = 6$). The arrows in (D)–(F) indicate the pulmonary granulomas (D), disorganization of WP and RP in spleen (E) and liver lesions (F).

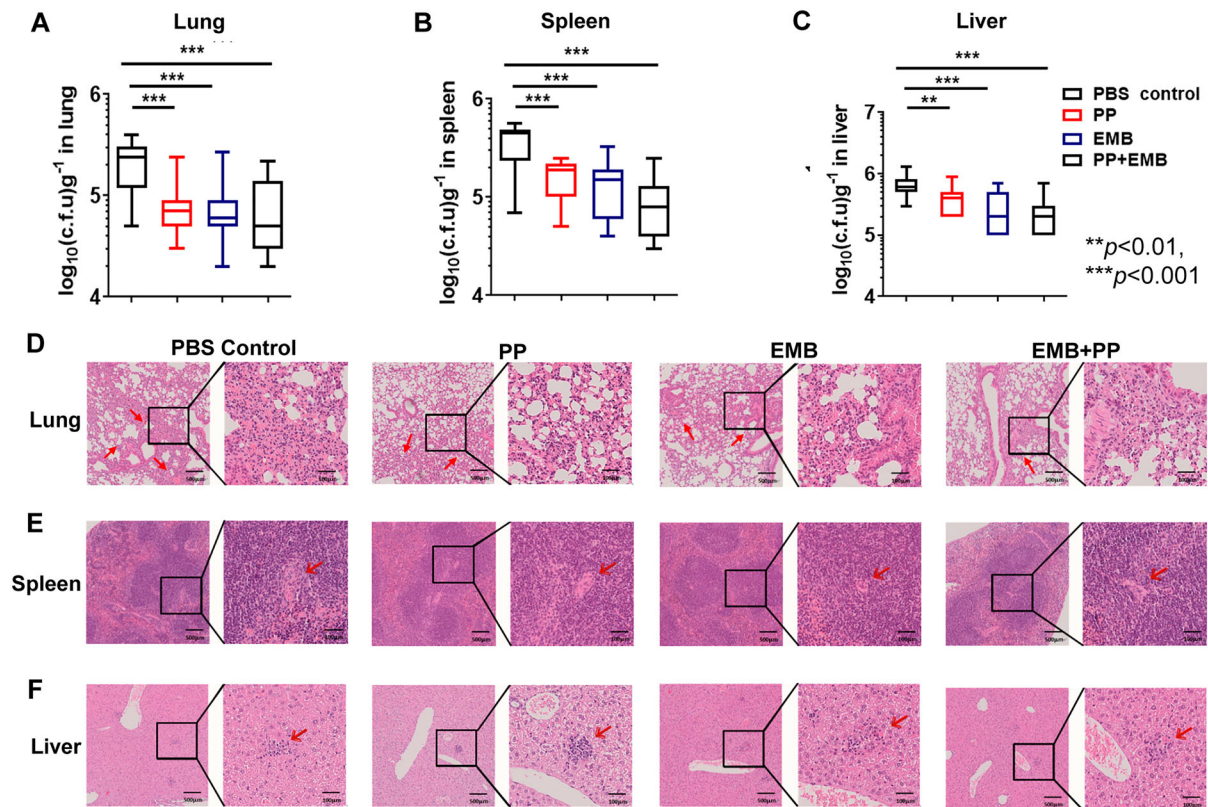


Figure 6. PP inhibits MDR *M. tb* 94789 growth in mice. The mice were infected (*i. v.*) with *M. tb* 94789 (1×10^4 CFU/mouse), and subjected to treatment with PP, EMB or PP in combination with EMB. After 4 weeks of therapy treatment, the bacterial loads in the lungs (A), spleens (B) and livers (C) were assessed. The pathological sections of lungs (D), spleens (E) and livers (F) were examined with H&E and evaluated by light microscopy. The data in (A)–(C) are shown as the means \pm SD ($n = 6$). The arrows in (D)–(F) indicate the pulmonary granulomas (D), disorganization of WP and RP in spleen (E), and liver lesions (F).

Because *M. tb* 94789 is RIF resistant, EMB treatment was used as a drug control. The mice were treated with PP, EMB or PP plus EMB on Week 0. After 4 weeks of treatment, both PP or EMB treatment significantly reduced the bacterial CFUs in lung, spleen and liver tissues compared with the PBS control group (Figure 6(A–C)), indicating that PP treatment inhibited MDR *M. tb* 94789 growth *in vivo* (Figure 6(A–C)). However, PP did not have a better antibacterial effect than EMB and there was no synergic effects between PP and EMB. Similarly, histological analysis revealed that PP treatment effectively reduced lesion and inflammation in lung, spleen and liver tissues by *M. tb* 94789 infection (Figure 6(D–F)).

In mouse model of *M. tb* 8462 infection, the mice were *i. v.* infected with *M. tb* 8462 on week -1 and treated with drugs on week 0. After 6 weeks of the treatment, compared with PBS control group, PP treatment significantly reduced the bacterial CFUs in lung, spleen and liver tissues, especially in liver, and had better anti-XDR *M. tb* 8462 effects than EMB did *in vivo* (Figure 7(A–C)). Moreover, PP plus EMB treatment decreased *M. tb* 8462 growth in the lung, spleen and liver tissues than EMB group, indicating there was a slight synergic effect between PP and EMB (Figure 7(A–C)). Histological analysis also revealed that PP treatment effectively reduced lesion and inflammation

in lung, introduced lymphoid hyperplasia in spleens and alleviated hepatocyte swelling, and displayed better protective effects than EMB did (Figure 7(D–F)).

Discussion

Studies have shown that in the last 40 years, only three new anti-TB drugs have been approved, namely Bedaquiline, Delamanid, and pretomanid worldwide [17–19]. The burden of TB and drug-resistant TB (DR-TB) continues to increase globally. 9% of DR-TB TB patients will develop MDR-TB even XDR-TB [2]. Both MDR-TB and XDR-TB are dangerous medical conditions that can affect patient outcomes, particularly mortality and TB control. Limited therapeutic drug options make the treatment of MDR-TB and XDR-TB difficult [20]. SOSA provides an attractive strategy, by which new potential pharmacological activity of an old approved drug may be identified. Although some new anti-malarial, antibacterial and antiviral drugs have been developed by SOSA [7–10,14,21–23], there is rarely reports about screening and identifying anti-*M. tb* drugs through this approach. In the present study, we used SOSA approach to screen out a new anti-*M. tb* drug, PP. We identified PP had remarkable inhibitory effects on *M. tb* and drug-resistant *M. tb* *in vitro* and *in vivo*.

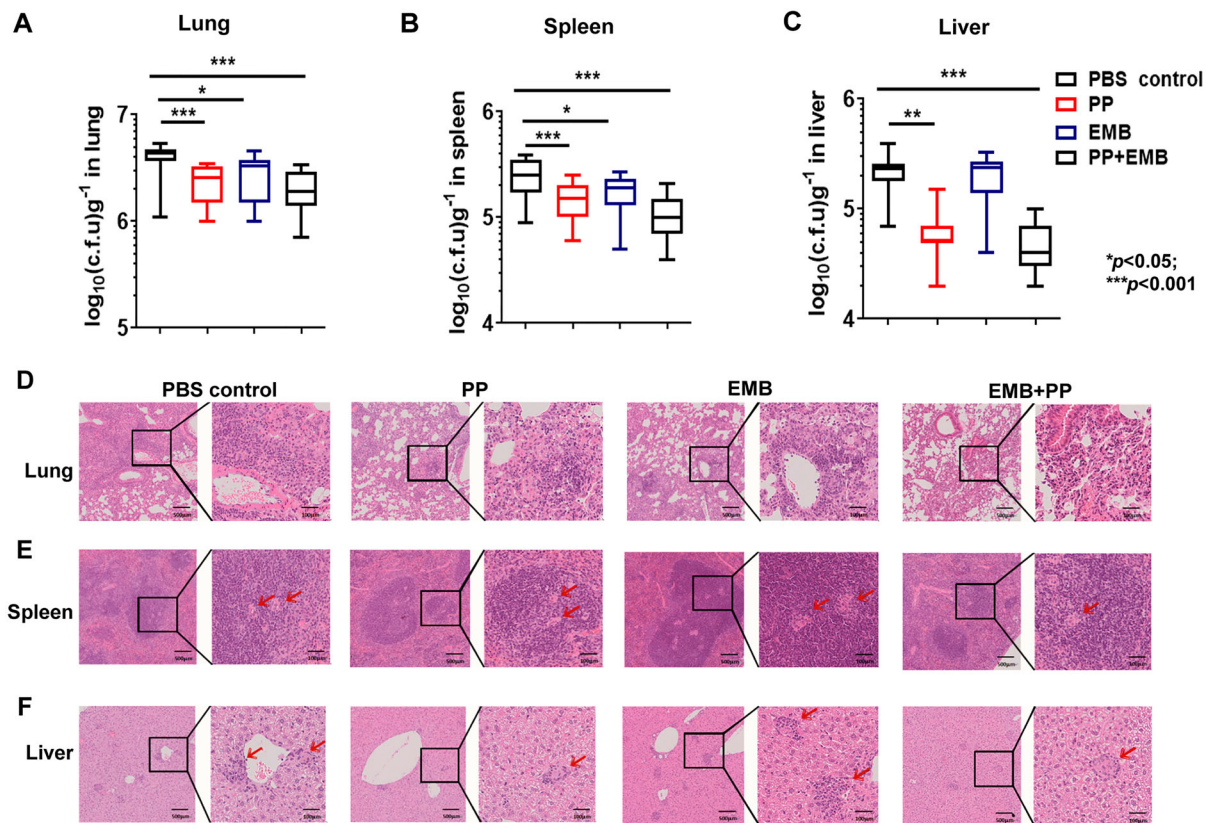


Figure 7. PP inhibits MDR *M. tb* 8462 growth in mice. The mice were infected (*i. v.*) with *M. tb* 8462 (1×10^5 CFU/mouse), and subjected to treatment with PP, EMB or PP in combination with EMB. After 6 weeks of therapy treatment, the bacterial loads in the lungs (A), spleens (B) and livers (C) were assessed. The pathological sections of lungs, spleens and livers were examined with H&E. The data in (A)–(C) are shown as the means \pm SD ($n = 6$). The arrows in (D)–(F) indicate the pulmonary granulomas (D), disorganization of WP and RP in spleen (E), or liver lesions (F).

M. smegmatis, BCG and *M. tb* H37Ra have a similar phenotype and characteristic to virulent *M. tb*. These mycobacteria have been commonly employed for screening anti-mycobacterial drugs [16,24]. In the current study, six candidate drugs (PP, BZK, meclizine hydrochloride, suloctidil, doxorubicin and teniposide) were selected from a library of known 1280 drugs and compounds using *M. smegmatis* as a target for the initial rapid screening. PP and BZK out of the six candidate drugs were identified to be capable of remarkably inhibiting the growth of BCG and *M. tb* H37Ra in a dose-dependent manner. PP had the lower MIC_{99} than BZK had, indicating that PP had the best anti-*Mycobacterium* effect among these drugs (Figure 2(B) and Table 2). Similarly, Kathryn et al used a medium-throughput assay using the Alamar Blue reagent to screen novel inhibitors of *M. tb* from a library of known 1514 drugs and also identified that five compounds including PP (Primaquine, Pentamide, Nialamide, PP, Thiostrepton and Isoniazid) were active against intracellular *M. tb* in a macrophage model of infection *in vitro* activity against *M. tb* H37Rv [25].

PP is a cyanine dye and is a classical anthelmintic officially approved by the FDA in 1955 (NDA-9582) [26]. When taken orally, the dose for human

commonly was 5 mg/kg/day, up to 350 mg, it is safe even at high doses, and its dose could be up to 35 mg/kg/day for 3–5 days [27,28]. As a drug against pinworm, the main role of PP is to interfere with the respiratory system of worms, inhibit the uptake of oxygen, increase the anaerobic glycolysis of sugar and impede the absorption of glucose, which causes the parasite to die, but does not kill the eggs [24,26,29]. This drug has been replaced by a more effective broad-spectrum anthelmintics in United States, but it is still employed in Europe and Japan [26]. It has been reported that PP inhibited the nicotinamide adenine dinucleotide (reduced form, NADH) in the respiratory chain and thus play an anti-tumor effect [30,31]. We speculated that PP inhibited the growth of *M. tb* by suppressing NAD^+/NADH conversion within the bacteria, but this requires further experimental validation. Recently, some studies reported that PP had pharmacological activity to inhibit the growth of *Bartonella henselae* infection [32] and coronaviruses replication *in vitro* [33,34]. PP has also been reported to have anti-tumor activity [28,34–37]. MIC values of *M. tb* H37Rv and *M. tb* 8462 are similar, however, in the murine model, PP activity against *M. tb* H37Rv is greater than against *M. tb* 8462 (Table 3 and Figure 7), possibly due to the complexity of *M. tb* 8462

pathogenesis *in vivo*. Further study is required to explore the mechanism of PP anti-mycobacterial activity.

Studies have shown that INH inhibits the growth of *M. tb* by suppressing the synthesis of mycolic acid, thus achieving the goal of treating TB [38]. RIF inhibits the growth of *M. tb* by binding the β subunit of RNA polymerase and suppressing transcription [39]. Therefore, the mechanism of PP inhibiting mycobacterial growth might be different from the antimycobacterial mechanisms mediated by INH and RIF. Consequently, PP showed its strong inhibitory effects on the growth of RIF-resistant, INH-resistant and even MDR-resistant *M.tb* clinical isolates *in vitro* (Figure 4(B–D)).

We hardly observed the *M. tb* H37Rv, *M. tb* 94789 and *M. tb* 8462 strains in the mouse lung tissue sections with Ziehl–Neelsen acid-fast stain, which is possibly due to less than 10^6 CFUs/g tissues during *M. tb* infection. Therefore, bacterial loads in the organs of infected mice were assessed by plating organ homogenates into medium and were determined by CFU counting (Figures 5–7). Although the amount of PP used in a murine model (0.5–1.5 mg/kg/day) is much lower than the amount of RIF and EMB used (20 and 100 mg/kg/day respectively), PP significantly inhibited the *M. tb* infection *in vivo* compared with PBS control groups (Figures 5–7), strongly demonstrating that PP had antimycobacterial activity *in vivo*. However without evaluation of antimycobacterial activity of PP at various concentrations *in vivo*, it is difficult to conclude which drug had the strongest anti-TB effects and whether PP had synergic effects with RIF (or EMB). Therefore, anti-TB function of various concentrations of PP should be investigated in a murine *M. tb* infection model in future studies.

In summary, three major observations were made in this study. First, PP was screened out as an anti-TB agent by SOSA and has remarkable inhibitory effects on the growth of multiple *M. tb* strains (including *M. tb* H37Rv, H37Ra, BCG) *in vitro*. Second, PP has anti-TB effects *in vivo*. Third, PP can also inhibit drug-resistant *M. tb* *in vitro* and *in vivo*. Our study may have far-reaching implications for the potential application of PP for the treatment of TB in the future.

Disclosure statement

No potential conflict of interest was reported by the author(s).

Funding

This work was supported by grants from the National Key R & D Program of China (2018YFA0507603), National Science and Technology Major Project of China (2017ZX10201301-006, 2012ZX10003002-015), National Natural Science Foundation of China (91740120, 21572173, 31770145 and 81971908), National Outstanding

Youth Foundation of China (81025008), the Major Projects of Technological Innovation of Hubei Province (2016ACA150), Natural Science Foundation Project of Hubei Province (2016CFA062), the Outstanding Youth Foundation of Hubei Province (2018CFA037), CAMS Innovation Funding For Medical Sciences (2016-I2M-2-006 and 2016-I2M-1-013), Medical Science Advancement Program (Basical Medical Sciences) of Wuhan University (TFJC 2018002) and the Hubei Province's Outstanding Medical Academic Leader Program (523-276003).

References

- [1] Daniel TM. The history of tuberculosis. *Respir Med.* 2006;100(11):1862–1870.
- [2] Global tuberculosis report. Geneva: World Health Organization; 2019.
- [3] Pezzella AT. History of pulmonary tuberculosis. *Thorac Surg Clin.* 2019;29(1):1–17.
- [4] Sukhithasri V, Vinod V, Varma S, et al. Mycobacterium tuberculosis treatment modalities and recent insights. *Curr Drug Deliv.* 2014;11(6):744–752.
- [5] Wermuth CG. Selective optimization of side activities: another way for drug discovery. *J Med Chem.* 2004;47(6):1303–1314.
- [6] Wermuth CG. Selective optimization of side activities: the SOSA approach. *Drug Discov Today.* 2006;11(3–4):160–164.
- [7] Gastaminza P, Whitten-Bauer C, Chisari FV. Unbiased probing of the entire hepatitis C virus life cycle identifies clinical compounds that target multiple aspects of the infection. *Proc Natl Acad Sci U S A.* 2010;107(1):291–296.
- [8] Imperi F, Massai F, Ramachandran Pillai C, et al. New life for an old drug: the anthelmintic drug niclosamide inhibits *Pseudomonas aeruginosa* quorum sensing. *Antimicrob Agents Chemother.* 2013;57(2):996–1005.
- [9] Lamontagne J, Mills C, Mao R, et al. Screening and identification of compounds with antiviral activity against hepatitis B virus using a safe compound library and novel real-time immune-absorbance PCR-based high throughput system. *Antiviral Res.* 2013;98(1):19–26.
- [10] van Cleef KW, Overheul GJ, Thomassen MC, et al. Identification of a new dengue virus inhibitor that targets the viral NS4B protein and restricts genomic RNA replication. *Antiviral Res.* 2013;99(2):165–171.
- [11] Weisman JL, Liou AP, Shelat AA, et al. Searching for new antimalarial therapeutics amongst known drugs. *Chem Biol Drug Des.* 2006;67(6):409–416.
- [12] Tang XL, Yuan CH, Ding Q, et al. Selection and identification of specific glycoproteins and glycan biomarkers of macrophages involved in *Mycobacterium tuberculosis* infection. *Tuberculosis (Edinb).* 2017;104:95–106.
- [13] Deng JH, Chen HY, Huang C, et al. Accumulation of EB13 induced by virulent *Mycobacterium tuberculosis* inhibits apoptosis in murine macrophages. *Pathog Dis.* 2019;77(1):ftz007.
- [14] An L, Liu R, Tang W, et al. Screening and identification of inhibitors against influenza A virus from a US drug collection of 1280 drugs. *Antiviral Res.* 2014;109:54–63.
- [15] Mekonnen A, Merker M, Collins JM, et al. Molecular epidemiology and drug resistance patterns of *Mycobacterium tuberculosis* complex isolates from

- university students and the local community in Eastern Ethiopia. *PLoS One*. 2018;13(9):e0198054.
- [16] Kumar S, Mehra R, Sharma S, et al. Screening of anti-tubercular compound library identifies novel ATP synthase inhibitors of *Mycobacterium tuberculosis*. *Tuberculosis (Edinb)*. 2018;108:56–63.
- [17] Gupta R, Wells CD, Hittel N, et al. Delamanid in the treatment of multidrug-resistant tuberculosis. *International Journal of Tuberculosis and Lung Disease*. 2016;20(12):S33–S37.
- [18] AlMatar M, AlMandael H, Var I, et al. New drugs for the treatment of *Mycobacterium tuberculosis* infection. *Biomed Pharmacother*. 2017;91:546–558.
- [19] Salinger DH, Subramoney V, Everitt D, et al. Population Pharmacokinetics of the Antituberculosis agent pretomanid. *Antimicrob Agents Chemother*. 2019;63(10):e00907-19.
- [20] Falzon D, Zellweger JP, Migliori GB, et al. Drug resistance and tuberculosis elimination in low-incidence countries. *Eur Respir J*. 2014;44(6):1408–1411.
- [21] Hsu JT, Yeh JY, Lin TJ, et al. Identification of BPR3P0128 as an inhibitor of cap-snatching activities of influenza virus. *Antimicrob Agents Chemother*. 2012;56(2):647–657.
- [22] Mao L, Wang J, DeGrado WF, et al. An assay suitable for high throughput screening of anti-influenza drugs. *PLoS One*. 2013;8(1):e54070.
- [23] Maroto M, Fernandez Y, Ortin J, et al. Development of an HTS assay for the search of anti-influenza agents targeting the interaction of viral RNA with the NS1 protein. *J Biomol Screen*. 2008;13(7):581–590.
- [24] Altaf M, Miller CH, Bellows DS, et al. Evaluation of the *Mycobacterium smegmatis* and BCG models for the discovery of *Mycobacterium tuberculosis* inhibitors. *Tuberculosis (Edinb)*. 2010;90(6):333–337.
- [25] Loughheed KE, Taylor DL, Osborne SA, et al. New anti-tuberculosis agents amongst known drugs. *Tuberculosis (Edinb)*. 2009;89(5):364–370.
- [26] Ishii I, Harada Y, Kasahara T. Reprofiled a classical anthelmintic, pyrvinium pamoate, as an anti-cancer drug targeting mitochondrial respiration. *Front Oncol*. 2012;2:137. doi:10.3389/fonc.2012.00137
- [27] Smith TC, Kinkel AW, Gryczko CM, et al. Absorption of pyrvinium pamoate. *Clin Pharmacol Ther*. 1976;19(6):802–806.
- [28] Xu W, Lacerda L, Debeb BG, et al. The antihelmintic drug pyrvinium pamoate targets aggressive breast cancer. *PLoS One*. 2013;8(8):e71508.
- [29] Simm C, May RC. Zinc and Iron Homeostasis: target-Based drug screening as New Route for Antifungal drug development. *Front Cell Infect Microbiol*. 2019;9:181. doi:10.3389/fcimb.2019.00181.
- [30] Tomitsuka E, Kita K, Esumi H. An anticancer agent, pyrvinium pamoate inhibits the NADH-fumarate reductase system—a unique mitochondrial energy metabolism in tumour microenvironments. *J Biochem*. 2012;152(2):171–183.
- [31] Tomitsuka E, Kita K, Esumi H. The NADH-fumarate reductase system, a novel mitochondrial energy metabolism, is a new target for anticancer therapy in tumor microenvironments. *Ann N Y Acad Sci*. 2010;1201:44–49.
- [32] Li T, Feng J, Xiao S, et al. Identification of FDA-approved drugs with activity against Stationary Phase *Bartonella henselae*. *Antibiotics (Basel)*. 2019;8(2):50.
- [33] Shen L, Niu J, Wang C, et al. High-Throughput screening and Identification of Potent broad-spectrum inhibitors of coronaviruses. *J Virol*. 2019;93(12):e00023-19.
- [34] Wiegering A, Uthe FW, Huttenrauch M, et al. The impact of pyrvinium pamoate on colon cancer cell viability. *Int J Colorectal Dis*. 2014;29(10):1189–1198.
- [35] Esumi H, Lu J, Kurashima Y, et al. Antitumor activity of pyrvinium pamoate, 6-(dimethylamino)-2-[2-(2,5-dimethyl-1-phenyl-1H-pyrrol-3-yl)ethenyl]-1-methylquolinium pamoate salt, showing preferential cytotoxicity during glucose starvation. *Cancer Sci*. 2004;95(8):685–690.
- [36] Xu L, Zhang L, Hu C, et al. WNT pathway inhibitor pyrvinium pamoate inhibits the self-renewal and metastasis of breast cancer stem cells. *Int J Oncol*. 2016;48(3):1175–1186.
- [37] Thorne CA, Hanson AJ, Schneider J, et al. Small-molecule inhibition of Wnt signaling through activation of casein kinase 1alpha. *Nat Chem Biol*. 2010;6(11):829–836.
- [38] Lei B, Wei CJ, Tu SC. Action mechanism of antitubercular isoniazid. Activation by *Mycobacterium tuberculosis* KatG, isolation, and characterization of inha inhibitor. *J Biol Chem*. 2000;275(4):2520–2526.
- [39] Xu M, Zhou YN, Goldstein BP, et al. Cross-resistance of *Escherichia coli* RNA polymerases conferring rifampin resistance to different antibiotics. *J Bacteriol*. 2005;187(8):2783–2792.